

Imprints of Early Universe Cosmology on Gravitational waves

arXiv: 2411.09757 [hep-ph]

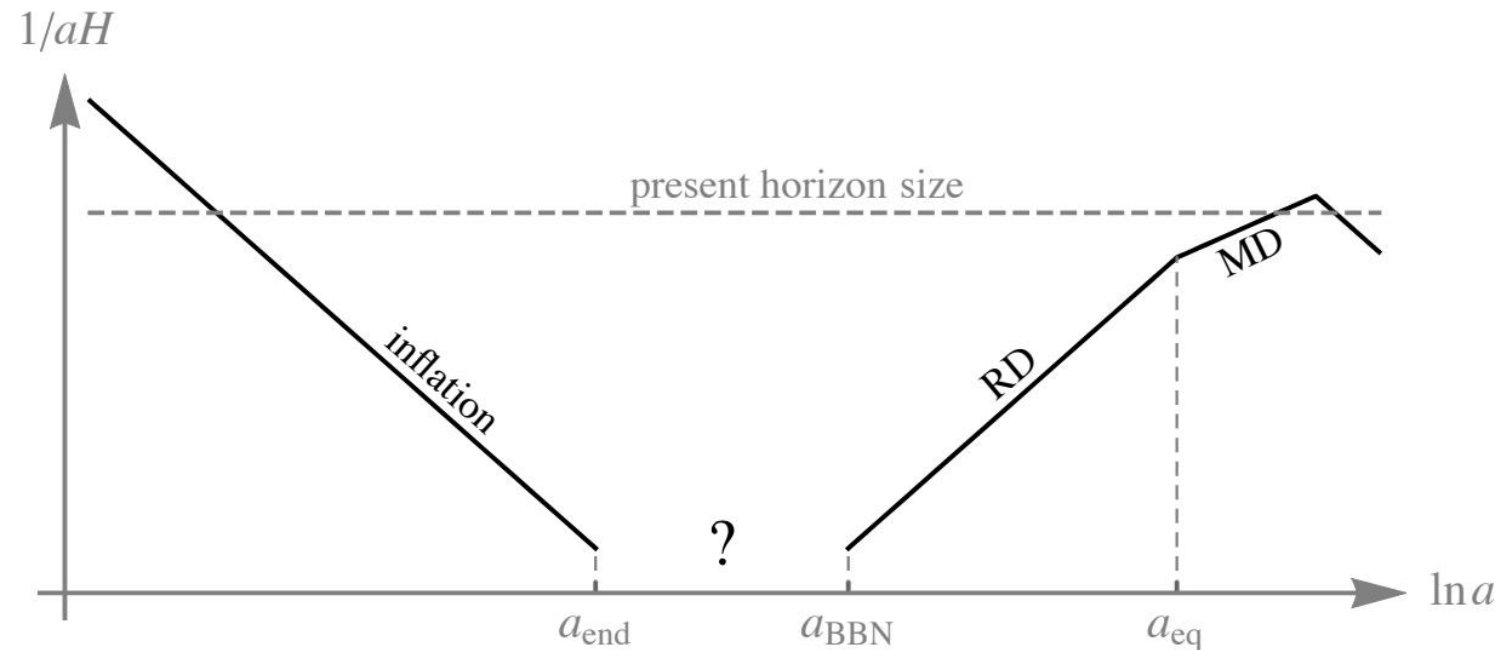
Mudit Rai

Texas A&M University

Collaborators : Bhaskar Dutta, James B. Dent

Motivation

- Physics before Big Bang Nucleosynthesis (BBN) ($T \sim \text{MeV}$) is not well understood due to lack of observational data.
- Gravitational waves can be a natural way to probe this epoch between end of inflation and BBN.



Cosmological setup

- ▶ We consider the scenario where the hidden sector is thermally decoupled to the SM.
- ▶ We assume that the SM makes up bulk of the energy density of the universe.
- ▶ The ratio of hidden sector temperature and that of SM is given by $\xi = \frac{T_h}{T_{SM}} < 1$ which also implies a hierarchy in the energy densities of the two sectors.
- ▶ Net energy density of the universe is given as, $\rho_R(T) = \frac{\pi^2}{30} \left(g_h^*(T) + \frac{g_{SM}^*(T_{SM})}{\xi^4} \right) T^4$

Energy injection

- ▶ Energy/entropy injection before BBN has been discussed extensively:
 - ▶ Fluctuations generated during inflation and later reentry [Carr & Lidsey,]
 - ▶ Collapse of domain walls [Cai et al, ...]
 - ▶ **PBH reheating** [Bernal et al, ...]
 - ▶ Bubble collisions during phase transition [Kodama et al, ...]
 - ▶ Temperature increase during reheating [Co et al, ...]
 - ▶ **Moduli decay** [Dutta et al...]
- ▶ The rate of energy injection can be either be fast where the field remains stuck as the temperature rises or can be slow where the field tracks its T dependent minima.

Impacts of energy injection

- ▶ The hierarchy in the two sectors imply that any small change in the energy density of the universe will impact the hidden sector more as compared to SM.
- ▶ The energy injection leads to an effective rise in hidden sector temperature

$$T \rightarrow \tilde{T} = T(1 + \delta)$$

- ▶ The energy injection can lead to multiple phase transitions in the hidden sector, and we will show that it can be probed by the associated GW spectrum.
- ▶ SM is dominant over the hidden sector implies,

$$\xi(1 + \delta) < \left(\frac{g_{SM}^*(T_i/\xi)}{g_h^*(T_i(1 + \delta))} \right)^{1/4}$$

Energy injection : Moduli decay

- The amount of energy injection to hidden sector via Moduli decay is given as,

$$\rho'_h = \rho_h + \rho_\chi$$

$$\implies T'_h = T_h \left(1 + \frac{30 m_\chi^2 \chi_i^2}{\pi^2 g_h^* T_h^4} \right)^{1/4}$$

- For hidden sector of $T_h \approx 100$ GeV and small delta,

$$\delta \approx 0.4 \left(\frac{m_\chi}{2.4 \times 10^8 \text{ GeV}} \frac{\chi_i}{4 \times 10^{-5} \text{ GeV}} \right)^2$$

- Larger initial field value leads to larger injection,

$$\delta \approx 4 \left(\frac{m_\chi}{2.4 \times 10^8 \text{ GeV}} \frac{\chi_i}{4.63 \times 10^{-4} \text{ GeV}} \right)^{\frac{1}{2}} - 1 \approx 3$$

Energy injection : PBH reheating

- ▶ Another instance for energy dumping to early universe happens via PBH evaporation.
- ▶ Following energy conservation before and after PBH evaporation, we get

$$T'_{SM} = T_{SM} \left(1 + \frac{\eta T_0}{T_{SM}} \right)^{1/4}$$

$$T'_h = T_h \left(1 + \frac{\eta T_0}{T_h} \right)^{1/4}$$

- ▶ For hidden sector of $T_h \approx 100$ GeV and small delta,

$$\delta \approx 0.45 \times \frac{\eta}{10^{-11}} \times \frac{0.1}{\xi} \times \left(\frac{M_{BH0}}{5.3 \times 10^4 g} \right)$$

- ▶ Larger initial mass fraction leads to larger injection,

$$\delta \approx 4 \left(\frac{\eta}{1.39 \times 10^{-9}} \times \frac{0.1}{\xi} \times \left(\frac{M_{BH0}}{5.3 \times 10^4 g} \right) \right)^{1/4} - 1$$

$\eta \equiv \frac{\rho_{BH}}{\rho_R} |_{T_0}$: Initial PBH mass fraction

Model realization

$$V \approx D(T^2 - T_0^2)\phi^2 - ET\phi^3 + \frac{\lambda}{4}\phi^4$$

- Initially, at high T , the field is in symmetric phase and there's just 1 minima at $\phi = 0$
- As universe cools, $T < T_1$, there exist a second minima

$$T_1^2 = \frac{T_0^2}{1 - \frac{9E^2}{8\lambda D}}, \quad \phi_1 = \frac{3ET_1}{2\lambda}$$

- As it further cools, these two minima become equi-potential and we have an onset of phase transition,

$$V(0, T_c) = V(\phi_c, T_c) \quad T_c^2 = \frac{T_0^2}{1 - \frac{E^2}{\lambda D}}, \quad \phi_c = \frac{2ET_c}{\lambda}$$

- After $T = T_0$, $\phi = 0$ ceases to be a minima and we are left with,

$$\phi_0 = \frac{3ET_0}{\lambda}$$

Criteria for three transitions

- For multiple transitions to occur due to the energy injection, following should be satisfied :

$$T_i < T_c < T_i(1 + \delta) < T_1$$

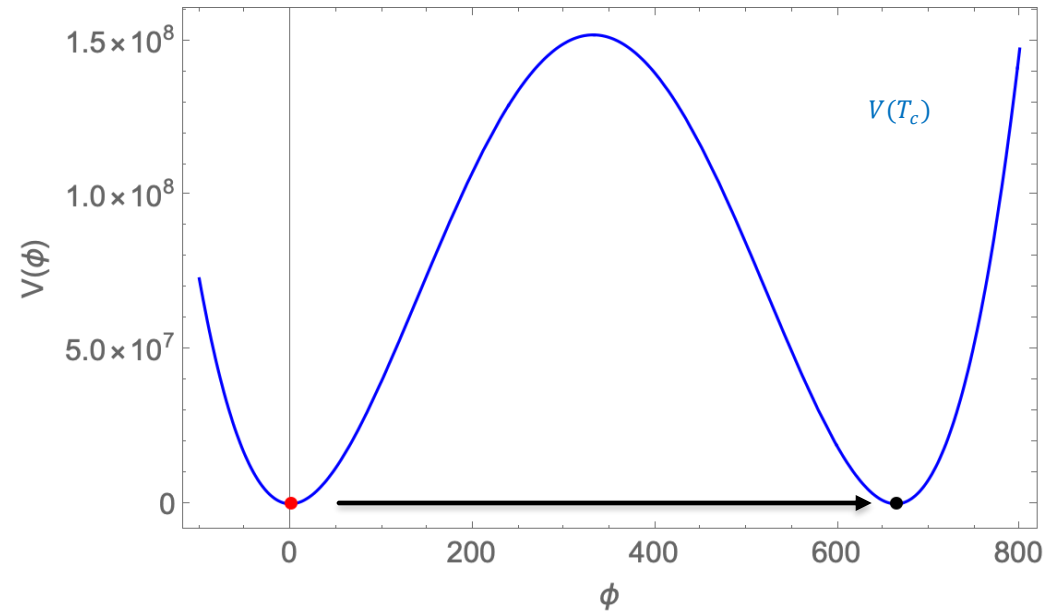
$$V(\phi_{min}(T_i(1 + \delta))) > 0$$

$$\phi_{max}(T_i(1 + \delta)) < \phi_i(T_i)$$

- In terms of model parameters,

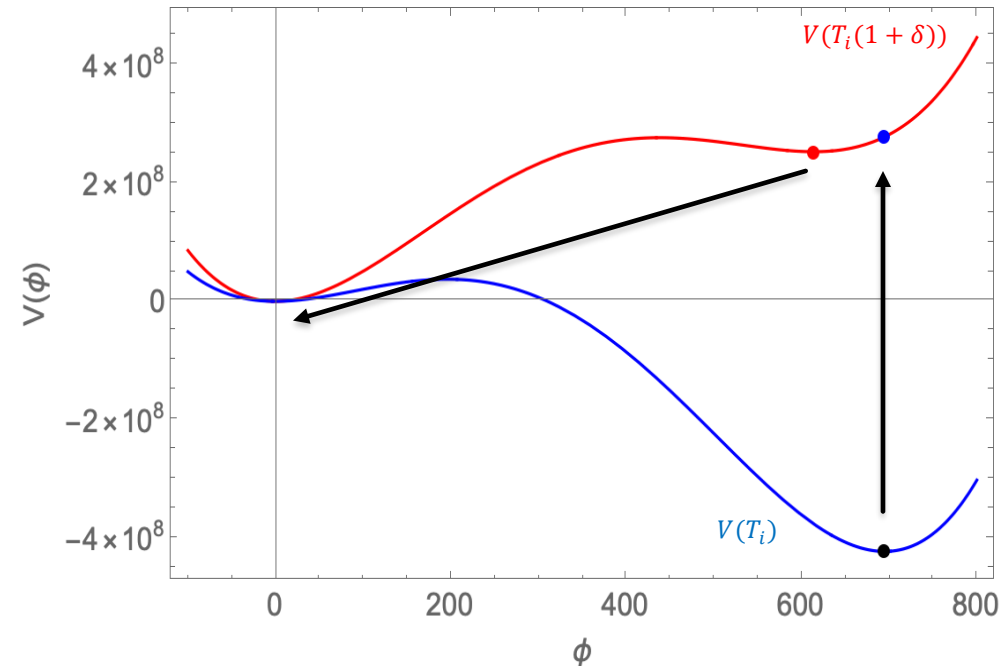
$$\eta := \frac{2\lambda D}{E^2} \in (9/4, 9/2)$$

Phase 1



- This transition corresponds to the standard scenario, where the field undergoes a PT $0 \rightarrow \phi_c$ when the two minimas become equipotential.

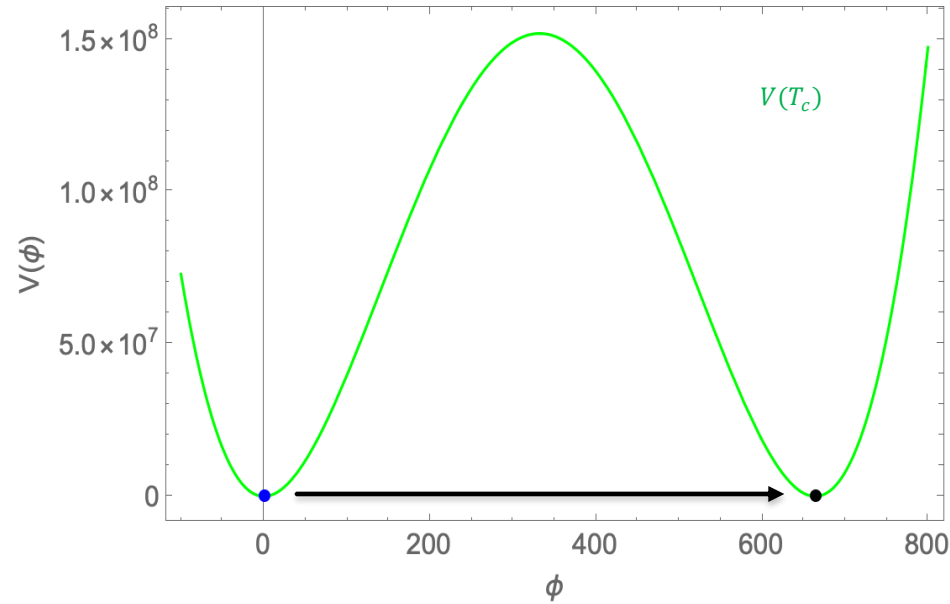
Phase 2



- In the broken phase, an energy injection, say at T_i , ($T_c > T_i > T_0$) will lead to $T_i \rightarrow T_i(1 + \delta) > T_c$
- Initially the field remains stuck¹ at $\phi_i(T_i)$ and eventually it rolls down to its T dependent minima $\phi_i(T_i(1 + \delta))$, leading to PT from $\phi_i \rightarrow 0$ (Phase 2).

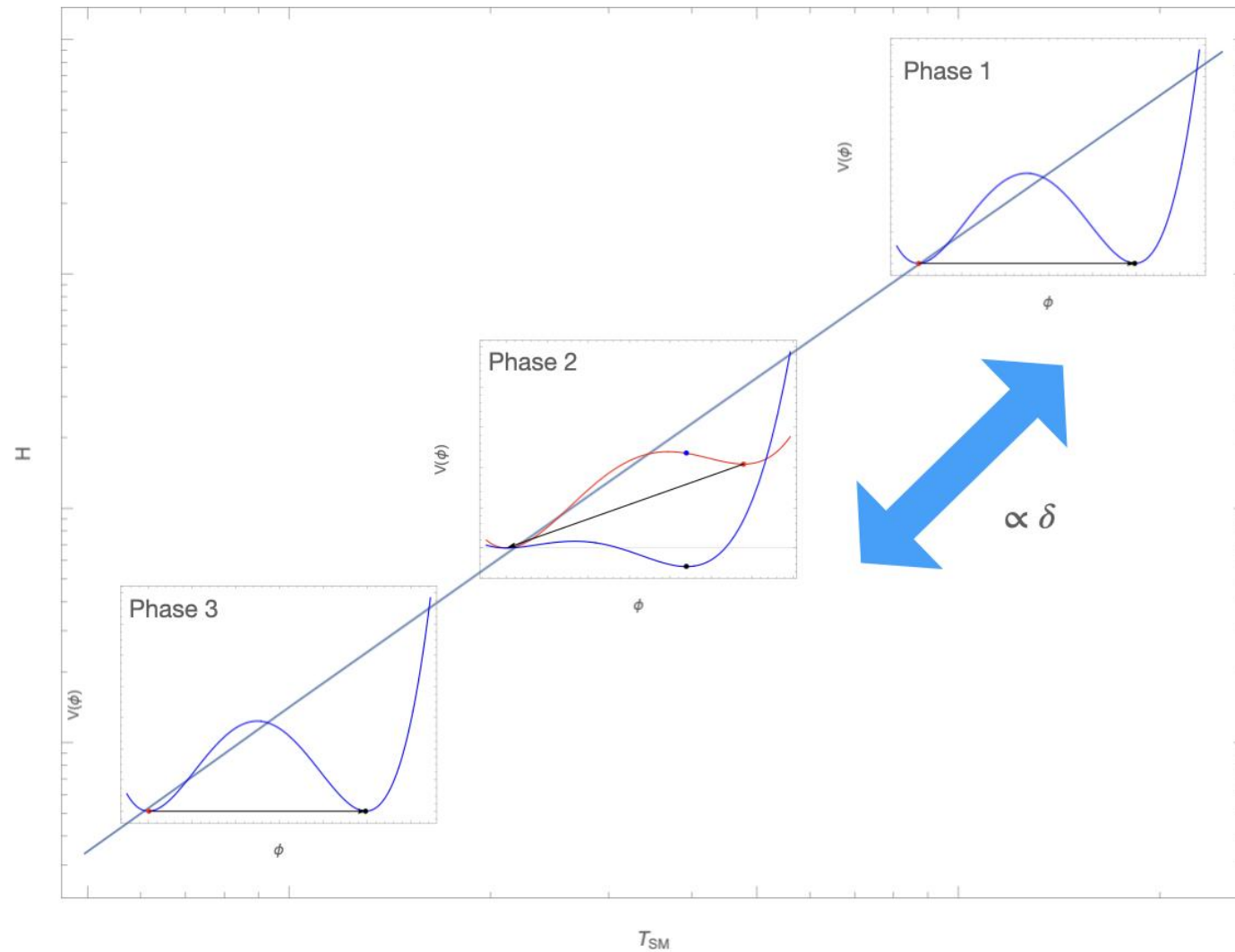
[1] Provided the rate of energy injection is large

Phase 3



- As universe cools down, there's another PT from $0 \rightarrow \phi_c$, which is like the standard transition but happens at later redshift (Phase III)
- For scenarios where hidden sector and SM have comparable energies, $\xi > 1$, Phase 1 and Phase 3 will become indistinguishable, similar to resetting the clock (Hubble).

Multiple transitions due to injection



Euclidean Action

- For simple polynomial like potentials, the Euclidean action determining the tunneling rate from a false vacuum state to the true vacuum state [Adams] ,

$$\frac{S_3}{T} \approx \frac{8E}{\lambda^{3/2}} f_S(\kappa(T)) \quad \kappa = \frac{2\lambda D(T^2 - T_0^2)}{E^2 T^2}, \quad 0 \leq \kappa \leq 2$$

$$f_S(x) = \frac{(8\pi\sqrt{x})(0.818x^3 - 5.533x^2 + 8.2938x)}{81(2-x)^2}$$

- For Phase II, we can modify the parameters accordingly as

$$\tilde{D} = D + \frac{3\phi_i(-2ET + \lambda\phi_i)}{2((T_i(1+\delta))^2 - T_0^2)} = D \left(\frac{9 - 4\kappa(\tilde{T}_i) + 3\sqrt{9 - 4\kappa(\tilde{T}_i)}}{2\kappa(\tilde{T}_i)} \right)$$

$$\tilde{E} = E - \frac{\lambda\phi_i}{T_i(1+\delta)} = E \left(\frac{1 + \sqrt{9 - 4\kappa(\tilde{T}_i)}}{2} \right)$$

$$\tilde{T}_i = T_i(\delta + 1)$$

$$\tilde{\kappa} = \frac{2\lambda\tilde{D}}{\tilde{E}^2} \left(1 - \frac{T_0^2}{T^2} \right) = \kappa(T) \left(\frac{9 - 4\kappa(\tilde{T}_i) + 3\sqrt{9 - 4\kappa(\tilde{T}_i)}}{\kappa(\tilde{T}_i)(5 - 2\kappa(\tilde{T}_i) + \sqrt{9 - 4\kappa(\tilde{T}_i)})} \right)$$

Nucleation Temperature and PT rate

- Nucleation temperature can be thought of as the temperature where a true vacuum bubble arise within a Hubble volume, i.e,

$$\Gamma/H^4 \approx 1$$

where,

$$\Gamma = T^4 \left(\frac{S_3}{2\pi T} \right)^{3/2} \exp^{-\frac{S_3}{2\pi T}}$$

- This simplifies as,

$$\left(\frac{S_3}{T} \right)_j \approx 173.7 - 2 \log g_{*,j} + 8 \log \xi_j - 4 \log \frac{T_0}{\text{GeV}} + 2 \log \left(1 - \frac{\kappa_{N,j}}{\eta} \right)$$

- Rate of the phase transition can be defined in terms of the Euclidean bounce action as,

$$\frac{\beta}{H_N} = T \frac{d(S_3/T)}{dT} \Big|_{T_N}$$

Strength of PT and wall velocity

- Amplitude of GW signal is controlled by strength parameter α :

$$\alpha = \frac{\Delta(V - \frac{1}{4}\partial_T V)}{\rho_R} \Big|_{T=T_N}$$

where $\Delta X = X_f - X_t$

- For wall velocity, we use analytical approximation[Ellis et al],

$$v_w = \begin{cases} \sqrt{\frac{\Delta V}{\alpha \rho_R}} & \sqrt{\frac{\Delta V}{\alpha \rho_R}} < v_J \\ 1 & \sqrt{\frac{\Delta V}{\alpha \rho_R}} > v_J \end{cases}$$

where

$$v_J = \frac{1}{1 + \alpha} \left(\sqrt{\frac{1}{3}} + \sqrt{\alpha \left(\frac{2}{3} + \alpha \right)} \right)$$

Gravitational Waves signal

- Differential GW density parameter characterizes them :

$$\Omega_{GW} = \frac{1}{\rho_c} \frac{d\rho_{GW}}{d \log f}, \quad \rho_c = 3M_{pl}^2 H^2$$

- Semi-analytical parametrizations can be used to describe them,

$$\Omega_{GW}(f) \simeq \sum_i \mathcal{N}_i \Delta_i(v_w) \left(\frac{\kappa_i \alpha}{1 + \alpha} \right)^{p_i} \left(\frac{H}{\beta} \right)^{q_i} s_i(f/f_{p,i})$$

$$\longrightarrow \Omega_{GW}^0(f) = \mathcal{R} \Omega_{GW} \left(\frac{a_0}{a} f \right)$$

$$\mathcal{R} \equiv \left(\frac{a}{a_0} \right)^4 \left(\frac{H}{H_0} \right)^2 \simeq 2.473 \times 10^{-5} h^{-2} \left(\frac{g_s^{\text{EQ}}}{g_s} \right)^{4/3} \left(\frac{g_\rho}{2} \right)$$

General features of Hidden sector PT

- ▶ $\alpha \propto \xi^4$ implies that for strong GW signals, Hidden sector and SM should have comparable temperature.
- ▶ Large β means faster transitions, which results in signals that are weaker and peaking at higher frequencies vs slower transitions.
- ▶ Larger ν_w implies smaller peak frequency and larger GW amplitude.
- ▶ Smaller T_N would lead to lesser redshift suppression.
- ▶ Smaller T_N/T_c is an indication of long-lasting phase transitions.

Relationship among phase 1 and 3

- Phase 1 and 3 are similar in nature, differing only due to redshift,

$$\kappa_3 \approx \kappa_1 + \chi, \quad \chi \ll 1$$

- Thus,

$$\left(\frac{S_3}{T}\right)_3 \approx \left(\frac{S_3}{T}\right)_1 + \frac{\chi(\beta/H)_1}{2(\eta - \kappa_1)}$$

$$\begin{aligned} \Rightarrow \kappa_3 &\approx \kappa_1 + \frac{16 \log(1 + \delta) (\eta - \kappa_1)}{(\beta/H)_1} \\ &\approx \kappa_1 + \frac{8 \log(1 + \delta)}{(S_3/T)_1 (\log(f_S(\kappa_1)))'} \end{aligned}$$

- This leads to

$$\frac{f_{p,obs,3}}{f_{p,obs,1}} \approx \sqrt{\frac{\eta - \kappa_{N,1}}{\eta - \kappa_{N,3}} \frac{f_\beta(\kappa_3)}{f_\beta(\kappa_1)}} \approx 1. \quad \alpha_{h,3}/\alpha_{h,1} \approx 1$$

Relationship among phase 2 and 3

- Actions between the two phases be related as

$$\left(\frac{S_3}{T}\right)_2 \approx \left(\frac{S_3}{T}\right)_3 \frac{f_S(\tilde{\kappa}(T, \tilde{T}_i))}{f_S(\kappa(T))} \left(\frac{1 + \sqrt{9 - 4\kappa(\tilde{T}_i)}}{2}\right)$$

where,

$$\frac{f_S(\tilde{\kappa}(T_{N,2}, \tilde{T}_i))}{f_S(\kappa_{N,3})} \approx 1 - \frac{2 \log\left(\frac{\eta - \kappa_{N,2}}{\eta - \kappa_{N,3}}\right)}{173.7 - 2 \log g_{*,3} + 8 \log \xi_f - 4 \log \frac{T_0}{\text{GeV}} + 2 \log\left(1 - \frac{\kappa_{N,3}}{\eta}\right)}$$

- The ratio of peak frequencies for the emitted GW is

$$\frac{f_{p,2,0}}{f_{p,3,0}} \approx \sqrt{\frac{\eta - \kappa_{N,3}}{\eta - \kappa_{N,2}}} \frac{\sqrt{9 - 4\kappa_i}}{\kappa_i} \left(\frac{\sqrt{9 - 4\kappa_i} + 3}{\sqrt{9 - 4\kappa_i} + 1}\right) \frac{f_\beta(\tilde{\kappa}(\tilde{T}_i, T_{N,2}))}{f_\beta(\kappa_{N,3})} \quad f_\beta(x) =: \frac{f'_S(x)}{6\pi}$$

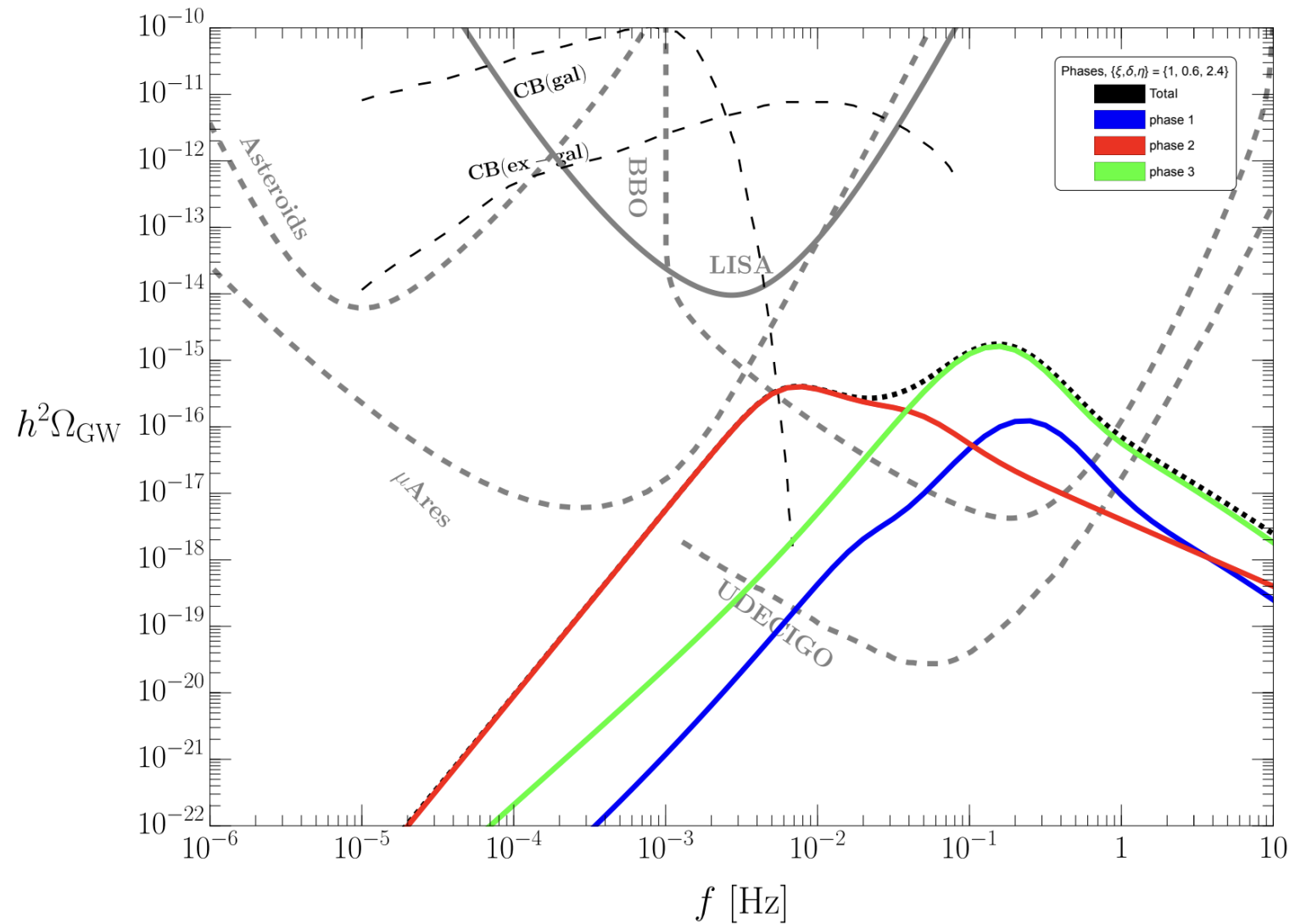
Impact of cosmology on GW

- The amplitude of GW for phase 1 vs phase 3 scales with amount of energy injected,

$$\frac{\Omega_{\text{GW},3,\text{obs}}^{(p)}}{\Omega_{\text{GW},1,\text{obs}}^{(p)}} \approx (1 + \delta)^6 \left(1 - \frac{8 \log(1 + \delta)}{(S_3/T)_1} g(\kappa_1, \eta) \right) \quad \frac{8 \log(1 + \delta)}{(S_3/T)_1} g(\kappa_1, \eta) \ll 1$$

- For phase 2 vs phase 3, we find that the amplitude ratio depends proportionally to the model parameter η in addition to ξ, δ .
- Knowing the peak frequency difference between phase 2 and 3 yields the value of $\xi(1 + \delta)$, in terms of model parameters and the scale of the hidden sector.

Results : $\xi = 1, \delta = 0.6, \eta = 2.4, T_0 = 450 \text{ GeV}$



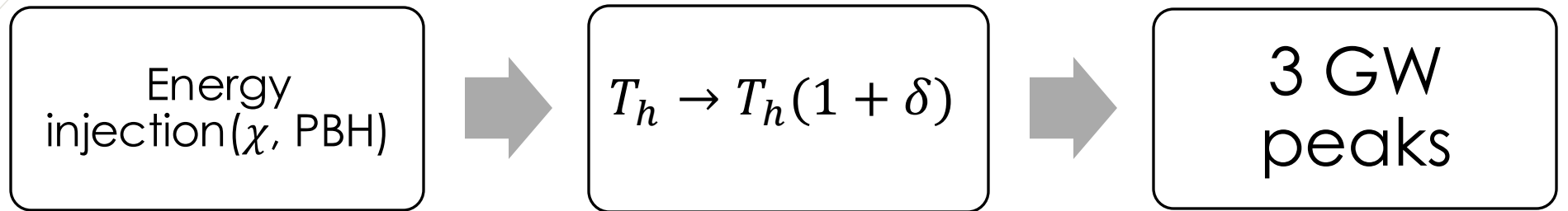
Results : $\xi = 0.75, \eta = 2.6, T_0 = 350 \text{ GeV}$

$\xi = 0.75$	α	β/H	α_h	T_N^{SM} (GeV)	f_P (Hz)	$h^2 \Omega_P$	κ
I	0.0009	1070.5	0.055	941.46	0.145	1.1×10^{-17}	1.546
II ($\delta = 0.57$)	0.002	429.8	0.017	839.3	0.09	2.5×10^{-17}	1.61
II ($\delta = 0.93$)	0.003	435.62	0.017	565.1	0.009	1.2×10^{-16}	1.62
III ($\delta = 0.57$)	0.006	1108.8	0.055	565.02	0.1	1.4×10^{-16}	1.55
III ($\delta = 0.93$)	0.01	1126.46	0.055	379.9	0.08	4.0×10^{-16}	1.55

Discussion

- ▶ Energy injection δ plays a significant role in shaping GW features.
- ▶ Larger energy injection δ leads to stronger GW amplitudes in phases 2 and 3 compared to phase 1, primarily due to smaller redshift suppressions, as shown in the tables.
- ▶ The tables verify that the peak frequencies ratios for phases 1 vs 3 are similar, differing from unity by a factor proportional to $\text{Log}(1 + \delta)$.
- ▶ The tables also verify the ratios for peak amplitude between phase 3 vs phase 1 scaling as $(1 + \delta)^6$.
- ▶ Smaller ξ leads to smaller peak amplitude due to weaker phase transition strength (α).

Conclusion



- ▶ Energy injection leads to more than one peak frequencies for GW from FOPT in hidden sector.
- ▶ For any reasonable ξ value (small or large), GW spectra have distinctive features due to multiple peaks.
- ▶ It is fairly independent w.r.to the mass scale of the hidden sector.
- ▶ Hidden sectors with GW can probe a variety of new physics scenario in the pre-BBN era.

THANK YOU!

BACKUP Slides

Phase 1 : Hydrodynamics

- Driving force for the PT in terms of the latent heat is,

$$\begin{aligned}
 F_{dr} &\approx \alpha \rho_R = \Delta \left(V - \frac{T}{4} \frac{dV}{dT} \right) \\
 &= \frac{T_N^2 \phi_c^2}{2\lambda} \left(\lambda D \frac{T_N}{T_c} - E^2 \right) > 0
 \end{aligned}$$

- The friction force is due to particles gaining mass as they go from the false vacua (symmetric phase) to the true vacua (broken phase).
- For runaway transition ($v_w \rightarrow c$), $F_{dr} > \Delta p_{LO}^{\gamma_w \rightarrow \infty}$ where,

$$\Delta p_{LO}^{\gamma_w \rightarrow \infty} \approx \sum_i \frac{c_i g_i (m_{t,i}^2 - m_{b,i}^2)}{24} > 0$$

- For most of our parameter space, we find that this happens to be a non-runaway transition, i.e, where the bubble wall never reaches the speed of light.

Phase 2 : Hydrodynamics

- ▶ The pressure difference due to mass difference is negative, since the particles loose mass as they pass from the false vacua (broken phase) to the true vacua (symmetrical phase).

$$\Delta p_{LO}^{\gamma_w \rightarrow \infty} \approx \sum_i \frac{c_i g_i (m_{t,i}^2 - m_{b,i}^2)}{24} < 0$$

- ▶ The force due to latent heat difference is also negative, and it acts as an effective friction.

$$F_{opp} \approx -T_i(1 + \delta) \eta (4 D T_i(1 + \delta) - 3 E \phi_i) - 2 D T_0^2 < 0$$

- ▶ This transition happens to be runaway¹, with the condition being

$$|\Delta p_{LO}^{\gamma_w \rightarrow \infty}| > |F_{opp}|$$

[1] For models without any production of soft vector bosons at the boundary

GW signal efficiency factors

- Turbulence efficiency factor can be estimated from sound wave as,

$$\kappa_{\text{Turb}} = \epsilon \kappa_{\text{SW}} ,$$

$$\epsilon = (1 - \min(H_* \tau_{\text{sh}}, 1))^{\frac{2}{3}}$$

- Sound wave efficiency factor differs in run-away vs non-runaway scenarios.
- For runaway scenarios, we have,

$$\kappa_{\text{SW}} = (1 - \kappa_{\text{BW}}) \frac{\alpha_{\text{eff}}}{0.73 + 0.083\sqrt{\alpha_{\text{eff}}} + \alpha_{\text{eff}}}, \quad \alpha_{\text{eff}} = \alpha_h (1 - \kappa_{\text{BW}})$$

- Efficiency factor for runaway in Phase 2 is based on numerical analysis in the works of Blasi et al on inverse transitions.

GW signal efficiency factors

- Sound wave efficiency factor for non-runaway transitions is:

$$\kappa_{\text{SW}} = \begin{cases} \frac{c_s^{11/5} \kappa_A \kappa_B}{(c_s^{11/5} - v_w^{11/5}) \kappa_B + v_w c_s^{6/5} \kappa_A}, & \text{if } v_w < c_s \\ \kappa_B + (v_w - c_s) \delta\kappa + \frac{(v_w - c_s)^3}{(v_J - c_s)^3} [\kappa_C - \kappa_B - (v_J - c_s) \delta\kappa], & \text{if } c_s < v_w < v_J \\ \frac{(v_J - 1)^3 v_J^{5/2} v_w^{-5/2} \kappa_C \kappa_D}{[(v_J - 1)^3 - (v_w - 1)^3] v_J^{5/2} \kappa_C + (v_w - 1)^3 \kappa_D}, & \text{if } v_J < v_w \end{cases}$$

with

$$\kappa_A \simeq v_w^{6/5} \frac{6.9 \alpha_h}{1.36 - 0.037 \sqrt{\alpha_h} + \alpha_h},$$

$$\kappa_B \simeq \frac{\alpha_h^{2/5}}{0.017 + (0.997 + \alpha_h)^{2/5}},$$

$$\kappa_C \simeq \frac{\sqrt{\alpha_h}}{0.135 + \sqrt{0.98 + \alpha_h}},$$

$$\kappa_D \simeq \frac{\alpha_h}{0.73 + 0.083 \sqrt{\alpha_h} + \alpha_h},$$

$$\delta\kappa \simeq -0.9 \log \frac{\sqrt{\alpha_h}}{1 + \sqrt{\alpha_h}}.$$

Results : $\xi = 1, \eta = 2.4, T_0 = 450 \text{ GeV}$

$\xi = 1$	α	β/H	α_h	T_N^{SM} (GeV)	f_P (Hz)	$h^2 \Omega_P$	κ
I	0.004	885.7	0.074	751.3	0.23	1.2×10^{-16}	1.545
II($\delta = 0.6$)	0.003	256.9	0.013	832.7	0.008	3.5×10^{-16}	1.61
II($\delta = 0.9$)	0.005	257.8	0.013	696.7	0.007	9.8×10^{-16}	1.615
III ($\delta = 0.6$)	0.018	909.9	0.071	477.3	0.15	1.5×10^{-15}	1.55
III ($\delta = 0.9$)	0.03	917.3	0.07	400.75	0.137	3.3×10^{-15}	1.55